

[2,2](5,8)Picenophanediene: Syntheses, Structural Analyses, Molecular Dynamics, and Reversible Intramolecular Structure Conversion

Min-Chih Tang,[§] Yu-Chen Wei,[§] Yen-Chen Chu, Cai-Xin Jiang, Zhi-Xuan Huang, Chi-Chi Wu, Tzu-Hsuan Chao, Pei-Hsun Hong, Mu-Jeng Cheng,* Pi-Tai Chou,* and Yao-Ting Wu*

Cite This: <https://dx.doi.org/10.1021/jacs.0c08115>

Read Online

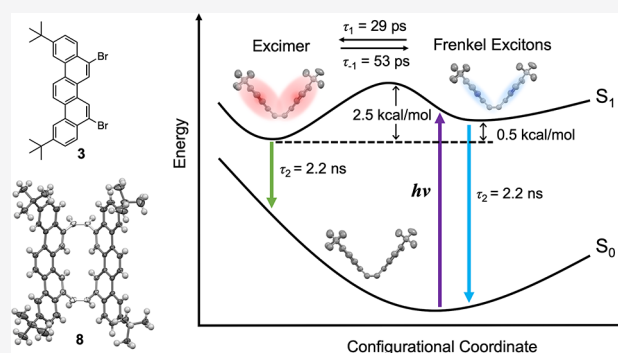
ACCESS |

Metrics & More

Article Recommendations

Supporting Information

ABSTRACT: This study presents an important and efficient synthetic approach to 5,8-dibromo-2,11-di-*tert*-butylpicene (**3**), with multigram scale, which was then converted to a new series of picenophanes (**6–10**). The tub-shaped [2,2](5,8)picenophanediene **8** with two *cis*-ethylene linkers was explored using X-ray crystallography. The tub-to-tub inversion proceed through the successive bending of the linkers and the barrier for isopropyl-substituted derivative **10** was experimentally estimated to be 18.7 kcal/mol. Picenophanes with a large π -system and semi-rigid structure exhibited anomalous photophysical properties. The ethano-bridged picenophane shows the weak exciton delocalization while the *cis*-ethylene-bridged picenophane exhibits dual emission rendered by the weakly delocalized exciton and excimer. With the aid of the ultrafast time-resolved emission spectroscopy, the mechanism of the excimer formation is resolved, showing a unique behavior of two-state reversible reaction with fast structural deformation whose lifetime is around 20 ps at 298 K. This work demonstrates that the slight difference in the bridge of tub-shaped picenophanes renders distinct photophysical behavior, revealing the potential of harnessing inter-moiety reaction in the picenophane systems.



INTRODUCTION

Dibenzo[*a,e*]cyclooctatetraene (DBCOT) and tetraphenylene are the simplest (double) tub-shaped arenes (TSAs, Figure 1) and are crucial ligands¹ and building blocks² in organic syntheses. Expanding π systems leads to the diversification of compound properties, as exemplified by cycloocta[1,2-*b*:5,6-

b']dianthracenes (CODA), which are photofunctional materials used as photoresponsive liquid crystals and light-melt adhesive.³ π -Extended derivatives, cycloocta[1,2-*b*:5,6-*b'*]ditetracene (CODT) and cycloocta[1,2-*b*:5,6-*b'*]dipentacene (CODP), exhibit characteristic excited-state photodynamics for attaining intramolecular singlet fission.⁴ Moreover, TSAs play major roles in supramolecular chemistry; for example, dicorannulene-fused tetraphenylene is a buckycatcher used to encapsulate a C₆₀ molecule.⁵ Enlarging the central ring size of DBCOT leads to the formation of cyclophanes,⁶ such as [2,2](2,7)naphthalenophanediene (NPD),⁷ [2,2](3,6)-phenanthro(2,7)naphthalenophanediene (PNPD),⁸ [2,2]-(3,6)phenanthrophanediene (PPD),⁹ [2.2](2,8)-dibenzothiophenophanediene (DBTPD),¹⁰ [2.2](3,10)benzo[*c*]phenanthrenophanediene (BPPD),¹¹ and [2.2](3,11)dibenzo[*a,j*]-anthracenophanediene (DBAPD).¹²

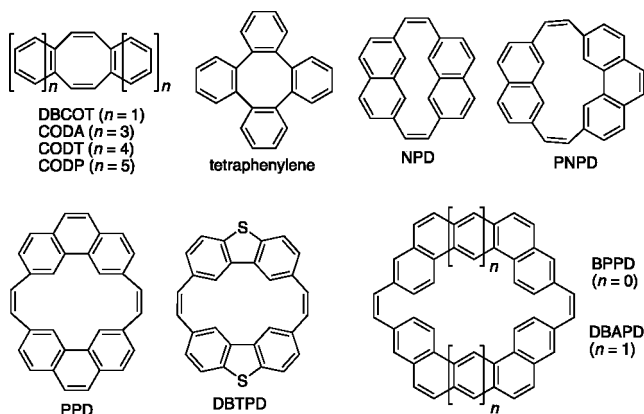


Figure 1. Ethylene-bridged cycloarenes and analogues.

Received: July 28, 2020

Except DBTPD, other cyclophanes were used as precursors for (attempted) syntheses of [8]carbon nanobelt and cycloarenes, including [*n*]circulenes and *Kekulene*, and their structures and properties have barely been explored. DBTPD with a quasi-planar structure, accompanied by some distortion in the central ring, is different from the aforementioned cyclophanes. PNPD⁸ and PPD⁹ were assigned to be tub-shaped (*syn*-conformers) based on theoretical investigations or chemical shifts in the ¹H NMR spectra, whereas NPD,^{7c} BPPD,¹¹ and DBAPD¹² were proposed to adopt step-like *anti*-conformers. Nonetheless, none of their structures were proved experimentally.

RESULTS AND DISCUSSION

Synthesis. In this study, a new series of picenophanes¹³ were synthesized, and their structures, molecular dynamics, and photophysical properties were explored. Despite several synthetic methods for preparations of picene^{14a,e} and 5,8-dihalopicene^{14e,f} being reported, efficient and hence gram-scale syntheses are still a great challenge.^{14g} Picenophanes may also suffer from low solubility in common organic solvents. Introduction of additional alkyl chains should improve the issue. Therefore, new synthetic approaches to *di-tert*-butyl-substituted picene and several picenophanes were investigated herein (Scheme 1). The Suzuki reaction of 4-bromo-2,3-dimethylphenyl triflate (1) with 2,4,6-tris(5-*tert*-butyl-2-methylphenyl)boroxin yielded 1,4-bis(5-*tert*-butyl-2-methylphenyl)-2,3-dimethylbenzene (2), which was converted into 5,8-dibromo-2,11-*di-tert*-butylpicene (3) on a multigram scale (2.32 g) through radical bromination with *N*-bromosuccini-

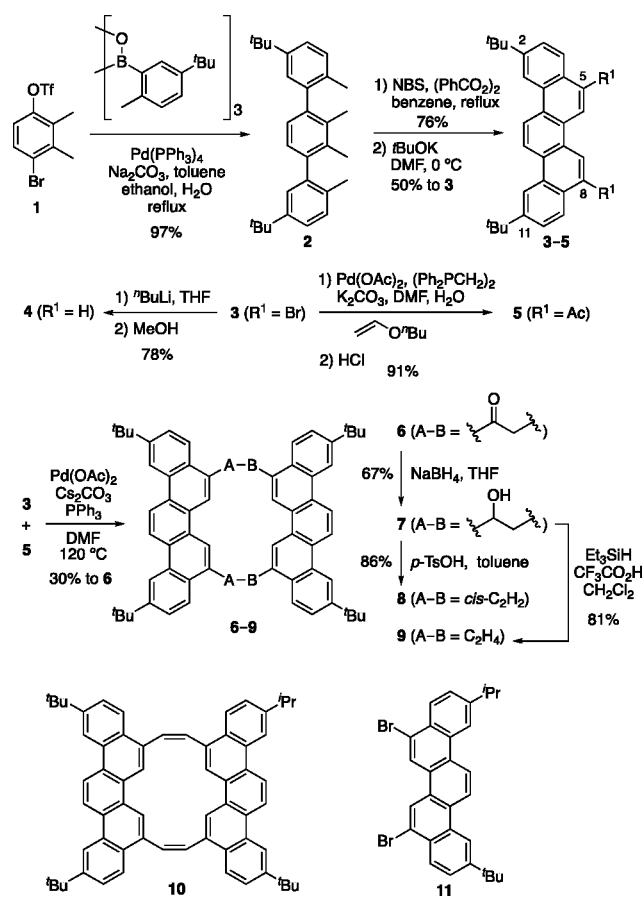
mide (NBS) and the subsequent base-mediated intramolecular couplings of benzylic (dibromo)methine (ArCHBr₂) and bromomethene (ArCH₂Br) of the thus generated hexabromo-substituted intermediate.¹⁵ Debromination of 3 through successive treatment with *n*-butyllithium and methanol produced 2,11-*di-tert*-butylpicene (4).

Next, how to effectively construct a cyclophane is equally important. NPDP,⁷ PNPD,⁸ BPPD,¹¹ and DBAPD¹² were synthesized from the corresponding dithiacyclophanes using a conventional route, which, regardless of chemical yields, required many essential synthetic steps, including methylation, oxidation, Stevens rearrangement, oxidation, and finally 1,2-Hofmann elimination or pyrolysis. Normally, PPD was achieved in 3–6 mg with small yields of 10–15% by photocyclization^{9a} or nickel-catalyzed cyclization^{9b} of halo-substituted [2.2.2]paracyclophanetraenes that were also acquired inefficiently. The aforementioned synthetic approaches thus may not be suitable for picenophanes. Alternatively, a new and efficient method was developed herein where flexible acetyl groups were used as linkers for connecting two picenyl moieties. Accordingly, palladium-catalyzed Heck reaction of 3 with *n*-butyl vinyl ether was conducted, which was followed by hydrolysis under acidic conditions to obtain 5,8-diacetyl-2,11-*di-tert*-butylpicene (5).¹⁶ Picenophane 6 was produced through palladium-catalyzed α -arylation¹⁷ of diketone 5 with an equal amount of 3. *cis*-Ethylene linkers in 8 and ethano bridges in 9 were prepared by reducing carbonyl groups of 6 and through the consecutive dehydration and dehydroxylation of the resulting compound, respectively. It needs to be emphasized that, with enough dibromopicene 3 in hand, the title compound 8 was accomplished on a semigram scale (415 mg). To study the molecular dynamics of [2,2](5,8)picenophanediene experimentally, isopropyl-substituted derivative 10 was prepared from 5 and 5,8-dibromo-2-*tert*-butyl-11-isopropylpicene (11) using the aforementioned synthetic method (see Scheme S1 in the Supporting Information).

Structural Analysis. Crystals of 6 and 8 were prepared through the slow diffusion of methanol in dichloromethane and chloroform solutions, respectively, at room temperature, and their diffraction data were collected at 100 K. The notable features of tub-shaped picenophane are mainly related to the arrangement of two picenyl moieties, as verified by the following structural parameters (see Figure 2a): (1) the dihedral angle between the mean square planes (θ_1) of the two picenyl moieties; (2) degree of staggering, determined using the torsion angle of a bridge (θ_2); (3) opening (d_1) and shrinking (d_2) of the tub, as estimated using the shortest interplanar distances between any two peripheral carbon atoms (C1, C2, C11, C12, C13, and C14) and inner carbon atoms (C5, C6, C7, and C8), respectively; and (4) the average of the distance (d_3) between the internal hydrogen atoms (H6...H6' and H7...H7').

Compound 6 crystallized in the monoclinic *P*₂₁/*c* space group, with oxygen atoms and one *tert*-butyl group being crystallographically disordered (Figure 2b). Moreover, 6 with flexible linkers was expected to exhibit two conformers *anti*-6 and *syn*-6. However, only *syn*-6 was obtained in the solid state, and the values of its structural parameters θ_1 , θ_2 , d_1 , d_2 , and d_3 were determined to be 103.2°, 83.1°, 9.092(3) Å, 3.345(3) Å, and 2.38 Å, respectively. According to the dihedral angle between the mean square planes of the first and fifth six-membered rings, one of the picenyl planes exhibited a higher

Scheme 1. Syntheses of Picenes and Picenophanes



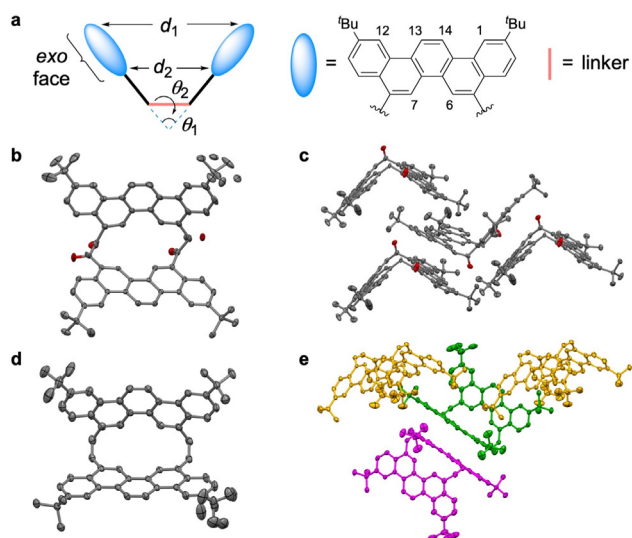


Figure 2. Structural parameters (a) and ORTEP drawings and molecular packing of **6** (b and c) and **8** (d and e) with 50% thermal ellipsoids. Hydrogen atoms are omitted for clarity.

degree of bending than did the other (13.3° vs 3.6°). The only *syn-6* conformer and its bent picene fragment were presumably caused by molecular packing. Each molecule **6** provided two *exo* picenyl faces for intermolecular $\pi\cdots\pi$ surface overlapping (Figure 2c) with numerous carbon–carbon nonbonded distances of $<3.434(3)$ Å (Figure S1 in the SI), which are comparable to the sum of the van der Waals radii of two carbon atoms (3.40 Å).^{18a} Several $\text{CH}\cdots\pi$ hydrogen bonds between the *tert*-butyl groups located in a cavity and concave faces were observed, and the shortest hydrogen bond exhibited a contact distance of 2.53 Å, which was measured as the distance between the concerned hydrogen atom and the centroid of the nearest six-membered ring.

Compound **8** with *cis*-ethylene linkers crystallized in the orthorhombic *Pbca* space group (Figure 2d), and its cavity was more rigid and smaller than that of **6**, as evidenced by the reduced values of θ_1 (76°), θ_2 (1.2°), d_1 [$7.321(4)$ Å], d_2 [$3.077(3)$ Å], and d_3 (2.33 Å). Similar to **6**, **8** crystallized with one crystallographically disordered *tert*-butyl group and a bent picenyl moiety of 17° . Molecules of **8** aggregated to form a quasi-one-dimensional supramolecular chain through $\text{CH}\cdots\pi$ interactions, where the concave π surface of the green molecule (see Figure 2e) attracted two *tert*-butyl groups of two yellow neighbors (one of each) to produce four hydrogen bonds with distances of 2.62–2.75 Å (Figure S2). The *exo*-faces of the two neighboring molecules (green and magenta) demonstrated $\pi\cdots\pi$ interactions. Effective overlapping was obtained mainly between the central biphenyls (second and fourth six-membered rings) of picenyl moieties; the separation of the mean square planes was 3.36 Å.

The structures of **8**, **9**, **10**, PPD and BPPD, and their molecular dynamics were theoretically examined using density functional theory¹⁹ (DFT, $\omega\text{B97XD}/6\text{-311g}^{**}$,²⁰ see the Supporting Information). The optimized geometry **8** obtained theoretically was consistent with that obtained experimentally. Picenyl moieties in the theoretically derived **8** were slightly bent (approximately 8°), and their structural parameters ($\theta_1 = 84^\circ$, $\theta_2 = 0.0^\circ$, $d_1 = 7.903$ Å, $d_2 = 3.095$ Å, and $d_3 = 2.149$ Å) were slightly different from those in the solid state. These distinct differences can be rationalized by perturbations of

intermolecular interactions. As expected, the calculated backbone of **10** is nearly identical to that of **8**. PPD has a tub-shaped structure similar to **8** and **10**. BPPD adopts a step-like *anti*-conformer, which is more stable than tub-shaped *syn*-conformer by 4.0 kcal/mol (Figure S3 and S8). The calculated structural parameters θ_1 , θ_2 , d_1 , d_2 , and d_3 of *syn-9* with C_2 symmetry are 83.9° , 71.6° , 8.743 Å, 3.293 Å, and 2.122 Å, respectively.

Molecular Dynamics. On the basis of DFT analyses, the tub-to-tub inversion of **8** to **8'** (= **8**) proceeded through the successive bending of the linkers via the transition state **8-TS**, the intermediate **8-Int**, in which one of the *cis*-ethylene linkers was oriented upward and the other was oriented downward from the backbone, followed by the transition state **8'-TS** (= **8-TS**, Figure 3). The barrier of the tub-to-tub inversion ($\Delta G_{\text{inv}}^\ddagger$)

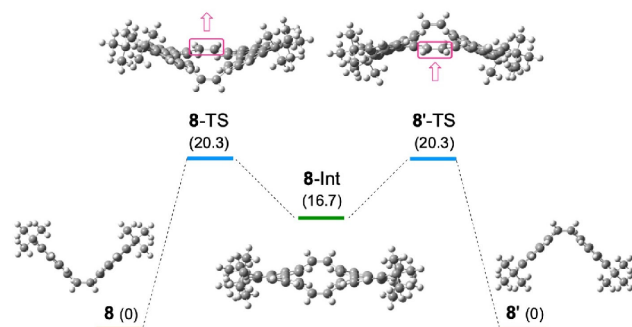


Figure 3. Energy profile for the ring-inversion process of **8**. The relative energies are reported in kcal/mol.

of **8** was estimated to be 20.3 kcal/mol. Several sterically congested positions were observed in **8-TS**, including one short nonbonded $\text{H}\cdots\text{H}$ contact (1.683 Å) in the inner ring and two pairs of *peri* hydrogen repulsions that distances between alkenyl hydrogen atoms and their neighboring aryl hydrogen atoms are 1.886 and 1.953 Å. The three values are smaller than the sum of the van der Waals radii of the hydrogen atoms (2.20 Å).^{18b} Experimentally, we then performed variable-temperature ^1H NMR studies of **10** in 1,2-dichlorobenzene- d_4 . The results revealed the occurrence of a slow tub-to-tub inversion at room temperature (Figure S5). Two sharp doublets of diastereotopic methyl groups (1.33 and 1.30 ppm, $\Delta\nu = 12.8$ Hz) at 293 K were converted into a well-resolved doublet (1.29 ppm) at 403 K. The coalescence temperature for signal merging was 358 K; hence, the value of $\Delta G_{\text{inv}}^\ddagger$ at the same temperature was approximately 18.7 kcal/mol, which agrees well with the calculated value (20.2 kcal/mol, see Figure S6). Unlike **8** and **10**, tub-to-tub inversions of CODA and PPD do not suffer from *peri* hydrogen repulsions and proceed via (quasi) planar transition states with barriers of 8.6³⁵ and 13.4 kcal/mol, respectively (Figure S7). We thus conclude that **8** and **10** are more rigid than CODA and PPD.

Upon cooling of the solution of **9** in CD_2Cl_2 (Figure S9), the signals of ^1H NMR spectra progressively split into two sets with a ratio of 1:1, which should be caused by C_2 -symmetric *syn-9*, the most stable conformer (see below). The barrier height (ΔG^\ddagger) for the dynamic process was experimentally determined as 11.8–12.6 kcal/mol at 243 or 253 K, depending on signals of different hydrogen atoms (Table S1). DFT calculations conclude that *syn-9*, which adopts a twisted tub-shaped structure, is more stable than *anti-9* by 4.2 kcal/mol (Figure 4). Therefore, signals of *anti-9* should not be observed

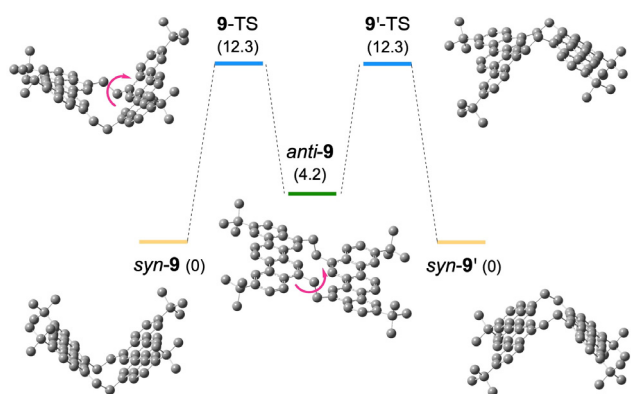


Figure 4. Energy profile for the ring-inversion process of **9**. The relative energies are reported in kcal/mol. Hydrogen atoms were omitted for clarity.

in the NMR spectra on a long time scale at the studied temperatures. *anti-9* is the intermediate for the inversion of *syn-9* to *syn-9'* (= *syn-9*). The conversion of *syn-9* to *anti-9* requires 12.3 kcal/mol, and the mechanism proceeded with a twisted V-shaped transition state **9-TS** through the successive rotation of the ethano linkers. Notably, [2,2](2,7)-naphthalenophane (NP),²¹ [2,2](3,6)phenanthro(2,7)-naphthalenophane (PNP)⁸ and [2,2](3,6)phenanthropane (PP)²² have been prepared (Figure 5), but the most stable conformer of only the first compound has been identified that *anti*-NP is more stable than *syn*-NP by 11.0 kcal/mol.

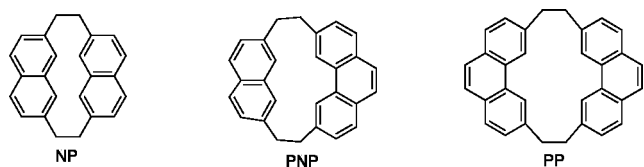


Figure 5. Ethano-bridged cyclophanes NP, PNP, and PP.

Electrochemical Properties. The redox properties of **4**, **8**, and **9** in dichloromethane were examined using cyclic voltammetry, and their reduction signals were not observed in this analytic window (Table S2 and Figure S10). Monomer **4** exhibited one irreversible oxidation wave with an onset potential of 0.90 V (vs the ferrocene/ferrocenium couple), indicating the low thermodynamic stability of the cationic species. The cyclic voltammograms of cyclophanes **8** and **9** are complex that their oxidation signals may contain multiple oxidation processes, verified by differential pulse voltammetry (DPV). The first oxidation potential of **9** (0.79 V) is lower than that of **8** (0.86 V). Compound **6** in tetrahydrofuran displayed one irreversible oxidation signal at 0.68 V, which exceeds that of **8** by 0.07 V.

Photophysical Properties. Table 1 and Figure 6 present the photophysical properties of the compounds. **4**, **8**, and **9** in cyclohexane exhibited similar absorption spectra, presumably because their frontier orbitals were mainly located at picenyl moieties with unremarkable orbital interactions (Figure 7). The π -orbital lobes of ethylene linkers in **8** were notable only in LUMO where they exhibited antibonding states. The HOMO–LUMO gaps (E_g^P) of **4**, **8**, and **9** were 3.54, 3.14, and 3.24 eV, respectively. On the other hand, the different vibronic progressive feature in the emission spectra of picenophane **9** and monomer **4** reveals the exciton delocalization in **9**. Based

Table 1. Photophysical Properties of Picenophanes and Their Fragments^a

	λ_{abs} (nm)	λ_{em} (nm)	Φ (%)	E_g^P (eV)
4	330, 350 (broad)	379, 400 ^b , 424 ^b , 449 ^b	6.5	3.54
8	386	386, 407 ^b , 435 ^b , 469, 496 ^b	2.7	3.14
9	363, 383 ^b	385, 406 ^b , 430 ^b , 458 ^b	13.3	3.24

^aMeasurements were conducted with samples (10 μM) in cyclohexane. Emission spectra were recorded with 330 nm excitation. The wavelengths of the absorption peak and the emission peak are denoted by λ_{abs} and λ_{em} , respectively. $\Delta\Phi$ and E_g^P are the quantum yields and the optical HOMO–LUMO gaps, respectively. ^bVibronic progression.

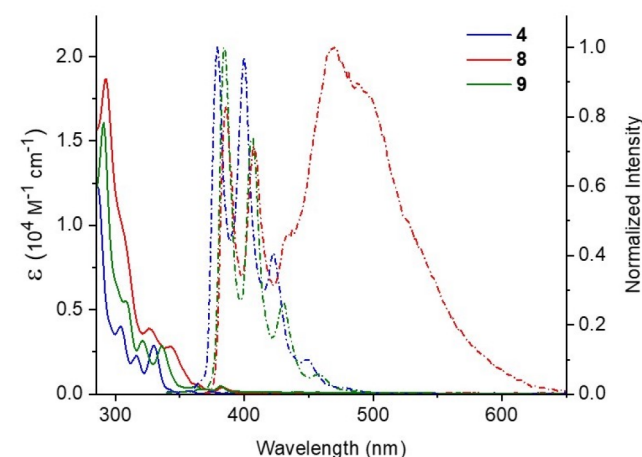


Figure 6. Absorption (left) and emission (right, λ_{ex} at 330 nm) spectra of **4**, **8** and **9** (1×10^{-5} M) in cyclohexane at 298 K.

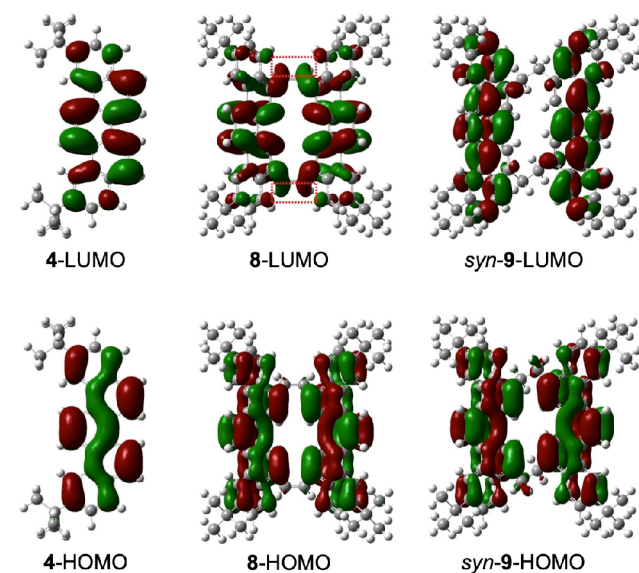


Figure 7. Frontier orbitals of **4**, **8**, and *syn-9*.

on the previous report,²³ the vibronic intensity ratio $I_{0 \rightarrow 0}/I_{0 \rightarrow 1}$ equals to N/λ^2 relating to the Huang–Rhys factor λ and delocalization number N . With this physical relation, the Huang–Rhys factor of monomer **4** is evaluated as 1.03. The slightly higher vibronic intensity ratio (1.36) in cyclophane **9** reflects that excitons delocalize at the picenyl moieties with $N \approx 1.36$, indicating weak intramolecular interaction between

two picene moieties in **9**. Such delocalization phenomena hold at 313 K–253 K in methylcyclohexane (Figure S11).

Importantly, picenophane **8** with *cis*-ethylene linkers demonstrates anomalous dual emission. The first emission band ranging from 380 to 420 nm (the F₁ band) resembles the emission profile of molecules **4** and **9**. Clearly, such an emission is attributed to the monomeric transition with slight exciton delocalization dubbed as Frenkel exciton states. In contrast, the broad emission band ranging from 450–650 nm (the F₂ band) is assigned as the excimer emission,²⁴ which is reminiscent of the emission of other diarylalkanes.²⁵ This assignment is firmly supported by the temperature-dependent emission spectra (Figure S12), showing that the excimer emission decreases with the lower temperature and disappears at 77 K in methylcyclohexane. This result indicates that such an emission band relates to the structural relaxation that is assisted by the thermal energy, matching the phenomena of excimer formation.

Comparing the dual emission and single emission bands for picenophanes **8** and **9**, respectively, the structure of the linker between the two picenyl moieties plays a key role for the excimer formation. A simple linker variation leads to much distinction in photophysics is surprising, which may be caused by different charge transfer coupling strength affected by the rigidity of the linker. The excimer emission of **8** is highly sensitive to the solvent polarity and viscosity (Figure S14). Toluene with relatively low dielectric constant ($\epsilon = 2.2$) and low viscosity ($\eta = 0.56$ cP at 298 K) causes the highest intensity ratio of excimer emission among the solvents studied herein. Cyclohexane with low dielectric constant ($\epsilon = 2.0$) and relatively high viscosity ($\eta = 0.86$ cP at 298 K, cf. toluene) and dichloromethane with high dielectric constant ($\epsilon = 8.9$) and low viscosity ($\eta = 0.40$ cP at 298 K) reduce the excimer emission ratio. Based on the observations, we surmise that the increase of the solvent viscosity hinders the structural relaxation incorporating large-amplitude motion, resulting in the less efficiency of the excimer formation. On the other hand, the energy level of the inter-moiety charge transfer state and the corresponding coupling strength may be affected by the increase of solvent polarity, which interfere the excimer formation. In other words, increasing either environmental polarity or viscosity decreases the excimer intensity. Thus, ratiometric emission for normal versus excimer can be harnessed by the interplay between viscosity and polarity. In contrast, the emission spectra of **9** are solvent-independent, indicating that the flexible ethano-bridge give more degrees of freedom for the structural variation, prohibiting the excimer formation.

To elaborate the dynamics of the picenyl system, the time-resolved emission spectroscopies combining the time-correlated single photon counting (TCSPC) and the femtosecond fluorescence upconversion are applied with the time resolution 20 ps and 150 fs, respectively. **4** and **9** show single exponential population decay with similar observed lifetimes (τ_{obs}) of 15 ns (Figure S15). With the information on Φ and τ_{obs} , the radiative decay rate constant (k_r) of **4** and **9** can be evaluated. As a result, k_r of picenophane **9** is deduced to be $8.7 \times 10^6 \text{ s}^{-1}$, which is around twice larger than that ($4.3 \times 10^6 \text{ s}^{-1}$) of monomer **4**. This result verifies the superradiance in picenophane **9**, echoing with the exciton delocalization of **9** confirmed by the larger $I_{0 \rightarrow 0}/I_{0 \rightarrow 1}$ in the steady-state emission spectra (vide supra).²³

As for the picenophane **8**, the transition between the Frenkel exciton state to the excimer state is captured (Figure 8 and

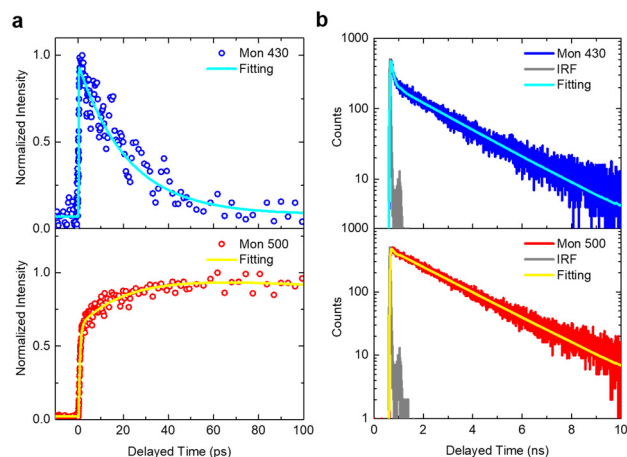


Figure 8. Time-resolved emission spectra of picenophane **8**. (a) Fluorescence up-conversion decay curves obtained in cyclohexane with an excitation wavelength (λ_{ex}) of 270 nm at 298 K. (b) TCSPC measurements in cyclohexane with λ_{ex} of 360 nm at 298 K.

Table 2. Fitting Lifetime of Picenophane **8 at 298 K^a**

λ_{mon} (nm)	observed lifetime τ_{obs} (pre-exponential factor)
430	18.6 ps (0.65), 2241 ps (0.35)
500	18.6 ps (−0.28), 2153 ps (0.72)

^a λ_{mon} is the monitored emission wavelength.

Table 2). Figure 8a demonstrates the corresponding rise-decay rate with τ_{obs} of 18.6 ps, representing the observed transition rate between Frenkel exciton and excimer states. In Figure 8b, the similar population decay lifetimes ($\tau_{\text{obs}} \approx 2.2$ ns) for both monomer and excimer emissions reveal the characteristic of pseudo-equilibrium between these two excited states. Such character indicates that the system here can be analogized as the two-state reversible reaction followed by excited-state dissipation (emission and non-radiative decay), which has been utilized to describe the dynamics of excited-state electron transfer,²⁶ proton-transfer²⁷ and proton coupled electron transfer.^{27,28} As a result, the equilibrium constant K_{eq} and the corresponding free energy difference ΔG can be derived by the ratio of the pre-exponential between fast and slow decay (see Figure 8), rendering $K_{\text{eq}} = 1.86$, $\Delta G = -0.5$ kcal/mol, which also roughly accords with the emission intensities between the Frenkel exciton state and excimer state. The relatively small ΔG with the large Stokes shift of the excimer emission (~ 13.6 kcal/mol) reflect that the redshift of the excimer emission should result from the common solvent relaxation of less than few picoseconds.

We further performed temperature-dependent dynamics of excimer formation. As a result, the slope of Arrhenius plot of the excimer formation rate (Figure S16) deduces an activation energy barrier (E_a) of 2.5 kcal/mol in methylcyclohexane. Such relatively small E_a comparing to the ones of the other diarylalkanes (3.4–4.2 kcal/mol) reveals that the *cis*-ethylene linker may play a crucial role in the suppression of E_a .^{25b,29} The results match well the shorter excimer formation lifetime of picenophane **8** at 298 K ($\tau = 29$ ps), which is much faster than

ones of the other diarylalkanes ($\tau = 10\text{--}100\text{ ns}$).^{25b,29,30} According to the extracted frequency factor ($1.13 \times 10^{12}\text{ s}^{-1}$), such short excimer formation lifetime could correlate to the low frequency vibronic motion of $\sim 40\text{ cm}^{-1}$. Based on the results elaborated above, the mechanism of excimer formation in picenophane **8** is summarized in Figure 9. Upon the

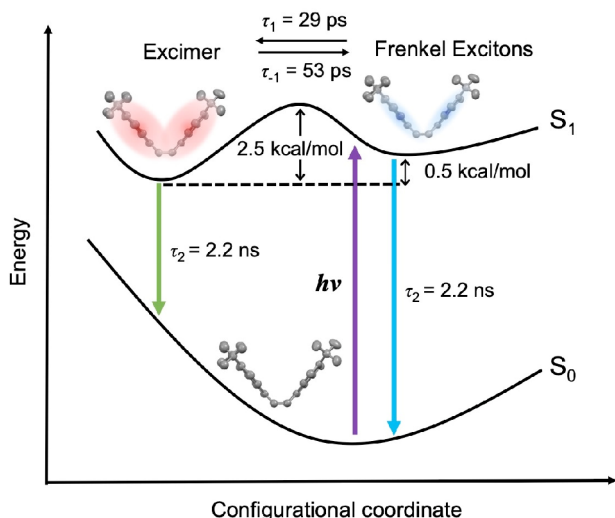


Figure 9. Excimer formation mechanism of picenophane **8**.

excitation of **8**, the Frenkel exciton immediately delocalizes to the two moieties. Subsequently, the population in the Frenkel exciton state transfers to the excimer state with lifetime $\sim 20\text{ ps}$ reversibly. The excited-state population then decays to the ground state with a lifetime 2.2 ns .

CONCLUSION

In summary, the chemistry, X-ray crystallographic structures, molecular dynamics, and photophysical properties of picenophanes were investigated. Tub-shaped [2,2](5,8)-picenophanediene with a large π -system and semirigid structure exhibited anomalous photophysical properties and photodynamics. Remarkably, we observed that slight difference in the bridge of the picenophane system renders significant change in the excited-state properties. Ethano-bridged picenophane **9** shows weak exciton delocalization verified by the vibronic progressive emission spectra and the superradiant effect. In sharp contrast, *cis*-ethylene-bridged picenophane **8** exhibits dual emission rendered by weakly delocalized exciton and excimer. The dynamics is elucidated by the time-resolved emission spectroscopy showing that the transition between Frenkel exciton and excimer states undergoes subtle structural deformation reversibly with a time constant of 18.6 ps (forward plus backward reactions) at 298 K , which is much faster comparing to the excimer formation rates of most diarylalkanes. This result together with the steady-state spectra indicates that the *cis*-ethylene linker contributes to not only the formation of excimer state in geometry but also the acceleration of excimer formation rate. The molecular design together with the comprehensive chemical analyses and insight into the photophysical properties sheds light on the unique excited-state behavior of tub-shaped picenophanes, providing a simple system to harness the inter-moiety reaction. The concave π surfaces of tub-shaped compounds **6** and **8** have the capability to form intermolecular hydrogen bonds with *tert*-

butyl groups. In the light of this information, accumulation of metals on the concave π surface of picenophane is ongoing in our laboratory, in order to explore metal- π and (potential) metal-metal interactions.³¹

ASSOCIATED CONTENT

Supporting Information

The Supporting Information is available free of charge at <https://pubs.acs.org/doi/10.1021/jacs.0c08115>.

Complete ref 19, experimental procedures, characterization data, computational studies, and X-ray crystallography data (PDF)

X-ray crystallographic data for **6** (CIF)

X-ray crystallographic data for **8** (CIF)

AUTHOR INFORMATION

Corresponding Authors

Yao-Ting Wu – Department of Chemistry, National Cheng Kung University, 70101 Tainan, Taiwan; orcid.org/0000-0001-7716-1855; Email: ytwuchem@mail.ncku.edu.tw

Pi-Tai Chou – Department of Chemistry, National Taiwan University, 10617 Taipei, Taiwan; orcid.org/0000-0002-8925-7747; Email: chop@ntu.edu.tw

Mu-Jeng Cheng – Department of Chemistry, National Cheng Kung University, 70101 Tainan, Taiwan; orcid.org/0000-0002-8121-0485; Email: mjcheng@mail.ncku.edu.tw

Authors

Min-Chih Tang – Department of Chemistry, National Cheng Kung University, 70101 Tainan, Taiwan

Yu-Chen Wei – Department of Chemistry, National Taiwan University, 10617 Taipei, Taiwan

Yen-Chen Chu – Department of Chemistry, National Cheng Kung University, 70101 Tainan, Taiwan

Cai-Xin Jiang – Department of Chemistry, National Cheng Kung University, 70101 Tainan, Taiwan

Zhi-Xuan Huang – Department of Chemistry, National Taiwan University, 10617 Taipei, Taiwan

Chi-Chi Wu – Department of Chemistry, National Taiwan University, 10617 Taipei, Taiwan

Tzu-Hsuan Chao – Department of Chemistry, National Cheng Kung University, 70101 Tainan, Taiwan

Pei-Hsun Hong – Department of Chemistry, National Cheng Kung University, 70101 Tainan, Taiwan

Complete contact information is available at: <https://pubs.acs.org/doi/10.1021/jacs.0c08115>

Author Contributions

[§]M.-C.T. and Y.-C.W. contributed equally to this work.

Notes

The authors declare no competing financial interest.

ACKNOWLEDGMENTS

This work was supported by the Ministry of Science and Technology of Taiwan (107-2113-M-006-013-MY3). The Instrumentation Center at National Tsing Hua University (X-ray crystallography), and the National Center for High-performance Computing (computational resources) are acknowledged.

REFERENCES

- (1) (a) Wender, P. A.; Lesser, A. B.; Sirois, L. E. Rhodium Dinaphthocyclooctatetraene Complexes: Synthesis, Characterization and Catalytic Activity in [5+2] Cycloadditions. *Angew. Chem., Int. Ed.* **2012**, *51*, 2736. (b) Singh, A.; Sharp, P. R. Platinum(II) and Palladium(II) Dibenz[*a,e*]cyclooctatetraene (DBCOT) Oxo and Halide Complexes: Comparison to 1,5-COD Analogues. *Organometallics* **2006**, *25*, 678. (c) Hiroi, Y.; Komine, N.; Komiya, S.; Hirano, M. Regio- and Enantioselective Linear Cross-Dimerizations between Conjugated Dienes and Acrylates Catalyzed by New Ru(0) Complexes. *Organometallics* **2014**, *33*, 6604. (d) Dzik, W. I.; Fuente Arruga, L.; Siegler, M. A.; Speck, A. L.; Reek, J. N. H.; de Bruin, B. Iridium Olefin Complexes Bearing Dialkylamino/amido PNP Pincer Ligands: Synthesis, Reactivity, and Solution Dynamics. *Organometallics* **2011**, *30*, 1902.
- (2) For selected examples, see: (a) Man, Y.-M.; Mak, T. C. W.; Wong, H. N. C. Synthesis of Benzo-Fused Tetraphenylenes and Crystal Structure of a 4:1 Clathrate Inclusion Compound of Dibenz[*b,h*]tetraphenylene with *p*-Xylene. *J. Org. Chem.* **1990**, *55*, 3214. (b) Pun, S. H.; Wang, Y.; Chu, M.; Chan, C. K.; Li, Y.; Liu, Z.; Miao, Q. Synthesis, Structures, and Properties of Heptabenz[7]-circulene and Octabenz[8]circulene. *J. Am. Chem. Soc.* **2019**, *141*, 9680. (c) Feng, C.-N.; Kuo, M.-Y.; Wu, Y.-T. Synthesis, Structural Analysis, and Properties of [8]Circulenes. *Angew. Chem., Int. Ed.* **2013**, *52*, 7791. (d) Miller, R. W.; Duncan, A. K.; Schneebeli, S. T.; Gray, D. L.; Whalley, A. C. Synthesis and Structural Data of Tetrabenz[8]circulene. *Chem. - Eur. J.* **2014**, *20*, 3705.
- (3) (a) Yuan, C.; Saito, S.; Camacho, C.; Irle, S.; Hisaki, I.; Yamaguchi, S. A π -Conjugated System with Flexibility and Rigidity That Shows Environment-Dependent RGB Luminescence. *J. Am. Chem. Soc.* **2013**, *135*, 8842. (b) Yamakado, T.; Otsubo, K.; Osuka, A.; Saito, S. Compression of a Flapping Mechanophore Accompanied by Thermal Void Collapse in a Crystalline Phase. *J. Am. Chem. Soc.* **2018**, *140*, 6245. (c) Saito, S.; Nobusue, S.; Tszaka, E.; Yuan, C.; Mori, C.; Hara, M.; Seki, T.; Camacho, C.; Irle, S.; Yamaguchi, S. Light-melt adhesive based on dynamic carbon frameworks in a columnar liquid-crystal phase. *Nat. Commun.* **2016**, *7*, 12094.
- (4) Yamakado, T.; Takahashi, S.; Watanabe, K.; Matsumoto, Y.; Osuka, A.; Saito, S. Conformational Planarization versus Singlet Fission: Distinct Excited-State Dynamics of Cyclooctatetraene-Fused Acene Dimers. *Angew. Chem., Int. Ed.* **2018**, *57*, 5438.
- (5) Sygula, A.; Fronczek, F. R.; Sygula, R.; Rabideau, P. W.; Olmstead, M. M. A Double Concave Hydrocarbon Buckycatcher. *J. Am. Chem. Soc.* **2007**, *129*, 3842.
- (6) For reviews on cyclophanes, see: (a) Hassan, Z.; Spuling, E.; Knoll, D. M.; Bräse, S. Regioselective Functionalization of [2.2]-Paracyclophanes: Recent Synthetic Progress and Perspectives. *Angew. Chem., Int. Ed.* **2020**, *59*, 2156. (b) Liu, Z.; Nalluri, S. K. M.; Stoddart, J. F. Surveying macrocyclic chemistry: from flexible crown ethers to rigid cyclophanes. *Chem. Soc. Rev.* **2017**, *46*, 2459. (c) Ghasemabadi, P. G.; Yao, T.; Bodwell, G. J. Cyclophanes containing large polycyclic aromatic hydrocarbons. *Chem. Soc. Rev.* **2015**, *44*, 6494. (d) *Modern Cyclophane Chemistry*; Gleiter, R.; Hopf, H., Eds.; Wiley-VCH: Weinheim, 2004.
- (7) (a) Davy, J. R.; Reiss, J. A. Synthesis of [2,2](2,7)-naphthalenophane-1,11-diene. *J. Chem. Soc., Chem. Commun.* **1973**, 806. (b) Davy, J. R.; Reiss, J. A. Cyclophanes. IV. Synthetic approaches to cyclophane dienes. The preparation of [2,2](2,7)-Naphthalenophane-1,11-diene. *Aust. J. Chem.* **1976**, *29*, 163. (c) Rioseras-garcia, M. J.; Hernando-huelmo, J. M. Theoretical conformational study of the stabilities and geometries of [2,2](2,7)-naphthalenophane-1,11-diene and related compounds. *Int. J. Quantum Chem.* **1994**, *52*, 651.
- (8) Jessup, P. J.; Reiss, J. A. Cyclophanes. VIII. An attempted preparation of [7]circulene from [2,2](3,6)Phenanthro(2,7)-naphthalenophane-1,11-diene. *Aust. J. Chem.* **1977**, *30*, 851.
- (9) (a) Thulin, B.; Wennerstrom, O.; Lindstrom, B.; Schaumburg, K.; Vialle, J.; Anthonsen, T. Synthesis of [2.2](3,6)-Phenanthrenophanediene. *Acta Chem. Scand.* **1976**, *30b*, 369. (b) Povie, G.; Segawa, Y.; Nishihara, T.; Miyauchi, Y.; Itami, K. Synthesis and Size-Dependent Properties of [12], [16], and [24] Carbon Nanobelts. *J. Am. Chem. Soc.* **2018**, *140*, 10054. (c) Liljefors, L.; Wennerstrom, O. Molecular mechanics calculations on the structures and conformational properties of [8]circulene and some related phane compounds. *Tetrahedron* **1977**, *33*, 2999.
- (10) Qiao, Y.; Wei, Z.; Risko, C.; Li, H.; Brédas, J.-L.; Xu, W.; Zhu, D. Synthesis, experimental and theoretical characterization, and field-effect transistor properties of a new class of dibenzothiophene derivatives: From linear to cyclic architectures. *J. Mater. Chem.* **2012**, *22*, 1313.
- (11) Staab, H. A.; Diederich, F.; Caplar, V. Cycloarenes, a New Class of Aromatic Compounds, III. Studies towards the Synthesis of Cyclo[*d.e.d.e.d.e.d.e.d.e*]decakisbenzene. *Liebigs Ann. Chem.* **1983**, *1983*, 2262.
- (12) (a) Staab, H. A.; Diederich, F. Cycloarenes, a New Class of Aromatic Compounds, I. Synthesis of Kekulene. *Chem. Ber.* **1983**, *116*, 3487. (b) Diederich, F.; Staab, H. A. Benzenoid versus Annulenic Aromaticity: Synthesis and Properties of Kekulene. *Angew. Chem., Int. Ed. Engl.* **1978**, *17*, 372.
- (13) Scifinder key words search (picenophane and cyclophane refined by picene) on July 1st, 2020 revealed that this class of compounds did not exist in the database.
- (14) (a) McAtee, C. C.; Riehl, P. S.; Schindler, C. S. Polycyclic Aromatic Hydrocarbons via Iron(III)-Catalyzed Carbonyl-Olefin Metathesis. *J. Am. Chem. Soc.* **2017**, *139*, 2960. (b) Xia, Y.; Liu, Z.; Xiao, Q.; Qu, P.; Ge, R.; Zhang, Y.; Wang, J. Rhodium(II)-Catalyzed Cyclization of Bis(*N*-tosylhydrazones): An Efficient Approach towards Polycyclic Aromatic Compounds. *Angew. Chem., Int. Ed.* **2012**, *51*, 5714. (c) Chang, N.-H.; Chen, X.-C.; Nonobe, H.; Okuda, Y.; Mori, H.; Nakajima, K.; Nishihara, Y. Synthesis of Substituted Picones through Pd-Catalyzed Cross-Coupling Reaction/Annulation Sequences and Their Physicochemical Properties. *Org. Lett.* **2013**, *15*, 3558. (d) Protti, S.; Artioli, G. A.; Capitani, F.; Marini, C.; Dore, P.; Postorino, P.; Malavasi, L.; Fagnoni, M. Preparation of (substituted) picones via solar light-induced Mallory photocyclization. *RSC Adv.* **2015**, *5*, 27470. (e) Okamoto, H.; Yamaji, M.; Gohda, S.; Kubozono, Y.; Komura, N.; Sato, K.; Sugino, H.; Satake, K. Facile Synthesis of Picene from 1,2-Di(1-naphthyl)ethane by 9-Fluorenone-Sensitized Photolysis. *Org. Lett.* **2011**, *13*, 2758. (f) Nakae, T.; Ohnishi, R.; Kitahata, Y.; Soukawa, T.; Sato, H.; Mori, S.; Okujima, T.; Uno, H.; Sakaguchi, H. Effective synthesis of diindinated picene and dibenzo[*a,h*]anthracene by AuCl-catalyzed double cyclization. *Tetrahedron Lett.* **2012**, *53*, 1617. (g) Carrera, M.; de la Viuda, M.; Guijarro, A. 3,3',5,5'-Tetra-*tert*-butyl-4,4'-diphenylquinone (DPQ)-Air as a New Organic Photocatalytic System: Use in the Oxidative Photocyclization of Stilbenes to Phenacenes. *Synlett* **2016**, *27*, 2783.
- (15) (a) Marcinow, Z.; Grove, D. I.; Rabideau, P. W. Synthesis of a New C₃₂H₁₂ Bowl-Shaped Aromatic Hydrocarbon: Acenaphtho[3,2,1,8-*ijklm*]diindeno[4,3,2,1-*cdef*:1',2',3',4'-*pqra*]triphenylene. *J. Org. Chem.* **2002**, *67*, 3537. (b) Goretta, S.; Tasciotti, C.; Mathieu, S.; Smet, M.; Maes, W.; Chabre, Y. M.; Dehaen, W.; Giasson, R.; Raimundo, J.-M.; Henry, C. R.; Barth, C.; Gingras, M. Expeditive Syntheses of Functionalized Pentahelicenes and NC-AFM on Ag(001). *Org. Lett.* **2009**, *11*, 3846.
- (16) Vallin, K. S. A.; Larhed, M.; Hallberg, A. Aqueous DMF-Potassium Carbonate as a Substitute for Thallium and Silver Additives in the Palladium-Catalyzed Conversion of Aryl Bromides to Acetyl Arenes. *J. Org. Chem.* **2001**, *66*, 4340.
- (17) Churrua, F.; SanMartin, R.; Carril, M.; Tellitu, I.; Domínguez, E. Towards a facile synthesis of triarylethanones: palladium-catalyzed arylation of ketone enolates under homogeneous and heterogeneous conditions. *Tetrahedron* **2004**, *60*, 2393.
- (18) (a) Pauling, L. *The Nature of the Chemical Bond*, 3rd ed.; Cornell University Press: Ithaca, 1960. (b) Rowland, R. S.; Taylor, R. Intermolecular Nonbonded Contact Distances in Organic Crystal Structures: Comparison with Distances Expected from van der Waals Radii. *J. Phys. Chem.* **1996**, *100*, 7384.

(19) Gaussian 09, revision A.02; Gaussian, Inc.: Wallingford, CT, 2016.

(20) Chai, J.-D.; Head-Gordon, M. Systematic optimization of long-range corrected hybrid density functionals. *J. Chem. Phys.* **2008**, *128*, 084106.

(21) Ohtsuka, K.; Cai, G.; Fujita, K.; Miyoshi, H.; Tobe, Y. Synthesis and structures of [2_n](2,7)naphthalenophanes (*n* = 2-4). *Can. J. Chem.* **2017**, *95*, 445.

(22) Thulin, B.; Wennerstrom, O. Synthesis and Photocyclization of [2.0.2.0]-, [2.2.2.0]- and [2.2.2.2]Cyclophanediene. *Acta Chem. Scand.* **1983**, *37b*, 297.

(23) Hestand, N. J.; Spano, F. C. Expanded Theory of H- and J-Molecular Aggregates: The Effects of Vibronic Coupling and Intermolecular Charge Transfer. *Chem. Rev.* **2018**, *118*, 7069.

(24) Tube-shaped [2.2](3,3')biphenyl(3,6)phenanthrene does not form excimer. For details, see: Nakamura, Y.; Tsuihiji, T.; Mita, T.; Minowa, T.; Tobita, S.; Shizuka, H.; Nishimura, J. Synthesis, Structure, and Electronic Properties of *syn*-[2.2]Phenanthrenophanes: First Observation of Their Excimer Fluorescence at High Temperature. *J. Am. Chem. Soc.* **1996**, *118*, 1006.

(25) (a) Chandross, E. A.; Dempster, C. J. Intramolecular excimer formation and fluorescence quenching in dinaphthylalkanes. *J. Am. Chem. Soc.* **1970**, *92*, 3586. (b) De Schryver, F. C.; Collart, P.; Vandendriessche, J.; Goedeweck, R.; Swinnen, A. M.; Van der Auweraer, M. Intramolecular excimer formation in bichromophoric molecules linked by a short flexible chain. *Acc. Chem. Res.* **1987**, *20*, 159. (c) Hirayama, F. Intramolecular Excimer Formation. I. Diphenyl and Triphenyl Alkanes. *J. Chem. Phys.* **1965**, *42*, 3163.

(26) Chen, K.-Y.; Hsieh, C.-C.; Cheng, Y.-M.; Lai, C.-H.; Chou, P.-T.; Chow, T. J. Tuning Excited-State Electron Transfer from an Adiabatic to Nonadiabatic Type in Donor-Bridge-Acceptor Systems and the Associated Energy-Transfer Process. *J. Phys. Chem. A* **2006**, *110*, 12136.

(27) (a) Tang, K. C.; Chang, M. J.; Lin, T. Y.; Pan, H. A.; Fang, T. C.; Chen, K. Y.; Hung, W. Y.; Hsu, Y. H.; Chou, P.-T. Fine Tuning the Energetics of Excited-State Intramolecular Proton Transfer (ESIPT): White Light Generation in A Single ESIPT System. *J. Am. Chem. Soc.* **2011**, *133*, 17738. (b) Liu, Z.-Y.; Hu, J.-W.; Chen, C.-L.; Chen, Y.-A.; Chen, K.-Y.; Chou, P.-T. Correlation among Hydrogen Bond, Excited-State Intramolecular Proton-Transfer Kinetics and Thermodynamics for -OH Type Proton-Donor Molecules. *J. Phys. Chem. C* **2018**, *122*, 21833.

(28) Cheng, C.-C.; Chang, C.-P.; Yu, W.-S.; Hung, F.-T.; Liu, Y.-I.; Wu, G.-R.; Chou, P.-T. Comprehensive Studies on Dual Excitation Behavior of Double Proton versus Charge Transfer in 4-(*N*-Substituted amino)-1H-pyrrolo[2,3-*b*]pyridines. *J. Phys. Chem. A* **2003**, *107*, 1459.

(29) (a) Zachariasse, K. A.; Maçanita, A. L.; Kühnle, W. Chain Length Dependence of Intramolecular Excimer Formation with 1,*n*-Bis(1-pyrenylcarboxy)alkanes for *n* = 1-16, 22, and 32. *J. Phys. Chem. B* **1999**, *103*, 9356. (b) Goldenberg, M.; Emert, J.; Morawetz, H. Intramolecular excimer study of rates of conformational transitions. Dependence on molecular structure and the viscosity of the medium. *J. Am. Chem. Soc.* **1978**, *100*, 7171.

(30) Snare, M. J.; Thistlethwaite, P. J.; Ghiggino, K. P. Nonlinear fluorescence quenching and the origin of positive curvature in Stern-Volmer plots. *J. Am. Chem. Soc.* **1983**, *105*, 3328.

(31) A preliminary study indicated that picenophane **8** should be a suitable ligand for metal cations. Treatment of a solution of **8** in chloroform with silver trifluoromethanesulfonate yielded [8•Ag]⁺ complex, which has been verified by mass spectra. Identification of the accurate coordination position is in progress.